Published in IET Renewable Power Generation
Received on 7th September 2007
Revised on 27th April 2008
doi: 10.1049/iet-rpg:20070091

ISSN 1752-1416

Aggregate modelling of wind farms containing full-converter wind turbine generators with permanent magnet synchronous machines: transient stability studies

J. Conroy R. Watson

University College Dublin, Ireland
E-mail: james.conroy@ucd.ie

Abstract: When the transient interaction between a large wind farm and a power system is to be studied, there are two possible approaches to wind farm modelling. It can be modelled as one or more equivalent wind turbine generators (aggregate modelling) or each wind turbine generator (WTG) can be modelled separately (detailed modelling). When a power system with many wind farms is to be simulated, the aggregate approach becomes especially attractive. A successful aggregate model will reduce the simulation time without significantly compromising the accuracy of the results in comparison to the detailed model. Here, the aggregate modelling options for a wind farm with 5 MW full-converter WTGs (FCWTGs) using permanent magnet synchronous machines are presented. A braking resistor in the DC circuit of the FCWTG's converter system is employed as a means of satisfying the latest grid code requirements. It will be shown that with a braking resistor implemented in the FCWTG there is scope for significant model simplifications, which is particularly relevant for transient stability studies of large-scale systems.

1 Introduction

The modelling of wind farms for grid integration studies is now an important issue, owing to the significant increase in connected wind power capacity [1]. In a power system model, a conventional generating plant will have each of its individual synchronous generators modelled separately. This does not significantly affect the simulation speed since the number of individual generators will be quite low. On the other hand, a wind farm will contain a large number of individual wind turbine generators (WTGs), possibly exceeding 100 for large offshore wind farms. Modelling each of these (WTGs) separately increases the complexity and compromises the simulation speed significantly. In a large power system that may contain a large number of wind farms, the need for aggregate wind farm models becomes obvious. An aggregate model that replaces a more detailed model should not significantly compromise the accuracy of the simulation results. This paper will look at the aggregate modelling options available (especially for transient stability studies) and comment on the accuracy thereof.

Grid code specifications in European countries require that wind turbines must be able to ride though grid disturbances that bring voltages down to very low levels. As an example, Fig. 1 shows the ride-through requirements in some European countries. The traces in Fig. 1 represent the grid code specifications of National Grid in England and Wales (E/W), Red Electrica in Spain (ESP), Eirgrid in Ireland (IRE) and E.On Netz in Germany (EON), respectively [2–5]. In the respective countries, wind farms must remain connected for a voltage dip above the respective critical line in Fig. 1. The grid code specifications in Ireland are particularly stringent. In addition to remaining connected, Eirgrid requires the wind farm to provide active power in proportion to retained voltage and to maximise its reactive power. Also, the wind farm must return to 90% of its

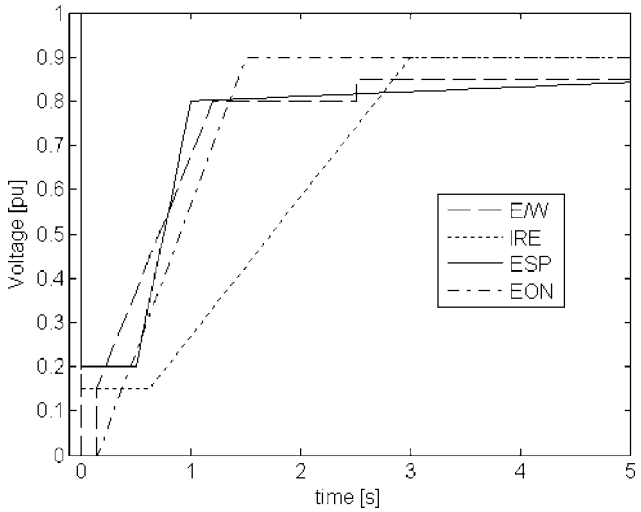

Figure 1 *Grid code fault ride-through specifications*

available active power output within 1 s of the fault ending. The requirements in the various countries have led to the development of the braking resistor technology for full-converter WTGs (FCWTGs), and it is employed by several manufacturers (e.g. Enercon GmbH [6]). Other methods of meeting, or attempting to meet, the requirements (such as converter blocking routines) are not considered in this work.

The wind farm modelled in this study contains 12 × 5 MW FCWTGs. The wind farm model is developed in the power systems simulation software package PowerFactory supplied by DIgSILENT GmbH [7]. Fig. 2 shows the power system model in PowerFactory. It will be shown that the effect of the braking resistor is such that the level of modelling detail required for an adequate aggregate model of this wind farm is significantly reduced.

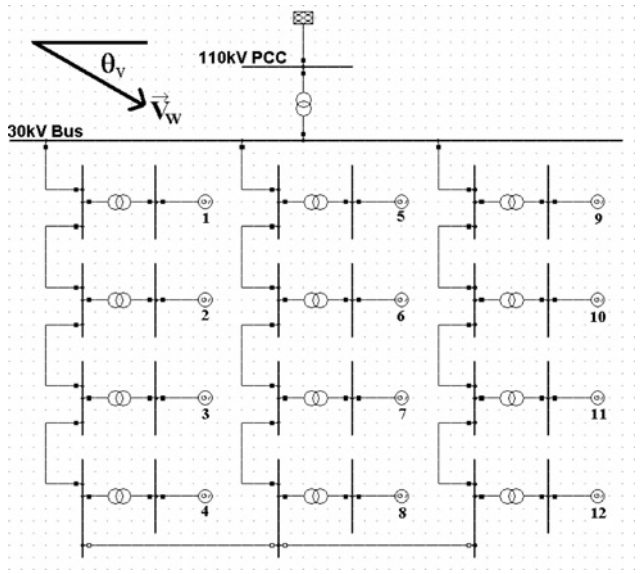

Figure 2 *PowerFactory diagram of the wind farm layout*

Some essential details on FCWTG modelling and control are presented initially. The aggregate modelling options are then presented. The simulation results will then show the considerable simplification in wind farm representation that is possible. Finally, ideas for future work in this area are proposed.

2 WTG model

The FCWTG studied in this paper uses a 40-pole-pair permanent magnet synchronous machine (PMSM) and a back-to-back pulse width modulation (PWM) voltage source converter system. The intermediate DC circuit of the converter system contains a capacitor and a braking resistor. Fig. 3 is an illustration of this system. The PMSM has 5 MW of active power capacity and the converter system is rated at full power since it connects the stator of the PMSM to the external network. The FCWTG modelled herein does not have a gearbox. Other designs may include a gearbox, reducing the required number of stator pole pairs, which would make the generator lighter and smaller. The important issue of gearbox reliability is then introduced, a significant disadvantage particularly for offshore applications.

The complete system of an FCWTG including the mechanical components, the electrical machine, the power electronic converters and the grid connection is a complex electromechanical system. A description of the components of the system model is now presented. The sequence of the described components follows the sequence of the energy conversion process. The braking resistor is inactive during normal operation, so its description is left to the end of this section.

2.1 Mechanical drive train

When WTGs are to be modelled for transient stability studies, it is typical to describe the energy extraction process from the wind as an algebraic relationship between the wind speed v_W and the extracted wind power P_W. This relationship is usually characterised by a set of aerodynamic efficiency curves $c_P(\lambda, \beta)$, where λ is the tip speed ratio and β the blade pitch angle [8].

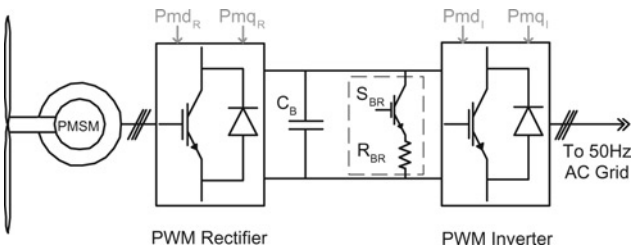

Figure 3 *Full-converter wind turbine with PMSM and back-to-back PWM converters*

doi: 10.1049/iet-rpg:20070091

The tip speed ratio λ is defined by

$$\lambda = \frac{\omega_T R}{v_W} \quad (1)$$

where ω_T is the rotational speed of the turbine. If the pitch angle β of the WTG does not change and the speed deviation is small, then it is valid to assume a constant extracted wind power P_W in the transient stability studies. This technique has been chosen in an aggregate model study in [9] giving good agreement with measured data for a fixed-speed wind farm. This approach is adopted herein. The drive train model used in this work is the *de rigueur* two-mass shaft model. This means that the turbine and PMSM inertias are represented separately, with a flexible coupling between them [10].

2.2 Synchronous machine

Equation (2) relates the speed ω_M in rpm of the PMSM to its output electrical frequency f_E in Hz

$$f_E = \frac{n}{120}\omega_M \quad (2)$$

Here n is the number of poles in the stator winding arrangement. The PMSM modelled herein has 80 poles. The FCWTG nominal speed is 15 rpm, meaning that the generator nominal frequency is 10 Hz since it is a gearless drive train. At wind speeds below the rated value, ω_M will be less than 15 rpm, so the electrical frequency f_E will be less than 10 Hz. According to (2), the relationship between these two parameters is linear. The PMSM is modelled using dq-axis theory, in a reference frame aligned with the rotor [11]. No damper windings are implemented in this machine.

It has been highlighted in previous publications [12, 13] that an FCWTG is prone to drive train oscillations. This is because with the large number of poles a small mechanical angle deviation leads to a large electrical angle deviation. Without proper control, a growing oscillation at the drive train natural frequency can occur. Control systems to prevent this have been analysed in [12–14]. In particular, it has been shown in [14] that the damping controller is not very relevant for transient stability studies of FCWTGs when braking resistors are employed. Hence, no discussion of damping controllers is included herein.

2.3 Voltage source converters

Referring to Fig. 3, the frequency converter is now described in detail. The electrical output of the PMSM has a low frequency: 10 Hz at rated power. This low frequency AC must be converted to 50 Hz AC so that it can be supplied to the power grid. A pair of back-to-back voltage source converters employing PWM are used to do this. The modulation index signals for the converters are shown in grey in Fig. 3. The first converter acts as a rectifier, converting the low-frequency AC to DC. The DC voltage is stabilised by the capacitor C_B in Fig. 3. The second converter acts as an inverter, with DC input and 50 Hz AC output that can be supplied to the grid.

In detailed variable-speed drive simulations, these converters are modelled using switch and snubber circuits for each switching device. A detailed representation of all the power electronic devices in an FCWTG would require a large number of state variables and a very small simulation step size (owing to the high switching frequency). The simulation time is greatly compromised in this case. The most obvious simplification to make is to use a fundamental frequency model for the converters with controlled voltage and current sources. This technique is widely used in variable-speed WTG stability research and it is accepted as the standard approach in this topic [15]. Such an approach is adopted herein. Harmonics and switching performance are of no interest in WTG stability analysis so this model is an attractive alternative to the detailed switch model.

2.4 Transformers and filters

The output current of the inverting converter will inevitably have some harmonic content. The most prominent harmonics can be predicted by considering the switching frequency and the modulation scheme [16]. So a filter is placed at the inverter's AC terminals to reduce the harmonic content at these frequencies. Each FCWTG has its own transformer (as indicated in Fig. 2), to connect it to the 30 kV voltage level of the wind farm cable network. Since the converters are modelled as fundamental frequency sources, the filters and transformers are represented herein by their fundamental frequency impedances only.

2.5 Braking resistor

When a transient event (such as a voltage dip) occurs in the power system, the terminal voltage of a WTG is reduced. In an FCWTG, this means that there is an excess of power in the DC link circuit that cannot be exported. A DC circuit braking resistor is used to dissipate this excess energy and restore the balance. This is known as 'electromagnetic braking' and it is a well-established technology in the field of variable-speed induction motor drives [16]. In variable-speed drives, this braking resistor balances output torque variations and prevents the DC link voltage from rising excessively. This resistor is typically controlled using a power electronic switch. Fig. 3 shows the positioning of this braking resistor R_{BR} and its controlling switch S_{BR} in the FCWTG.

In a stability model of an FCWTG, it is not practical to include a detailed power electronic switch model (for S_{BR} in Fig. 3) or a resistor model with parasitic effects (such as its inductance). In this paper, ideal switch and ideal resistor models are used. Hence, the switch and resistor

doi: 10.1049/iet-rpg:20070091

combination can be modelled as a controlled current source in the DC link circuit. This is quite convenient, since the value of current for this current source can simply be added to that of the DC current source of the grid-side inverter model: so no new element is needed in the circuit model.

3 FCWTG control system

The control system for any WTG has as its principal objectives the maximisation of the energy capture from the wind, robustness to power system disturbances (such as voltage dips) and protection of the various components from damage. The following is a description of the control system components that are pertinent in this aggregate modelling study.

3.1 Converter control

The converter controllers are used to regulate the converter currents and voltages and the active and reactive power output of the FCWTG. Fig. 4 shows the outline of the control scheme for the machine-side rectifying converter. The rectifying converter is used to control the generator AC voltage V_{ACG} and the output active power P_{G} of the PMSM. The PI controllers for V_{ACG} and P_{G} define reference values for the dq-axis components $i_{d\mathrm{R}}$ and $i_{q\mathrm{R}}$ of the rectifier AC current. The dq-axis components are in a reference frame oriented with the rectifier AC voltage. The inner PI controllers define the dq-axis modulation indices $P_{\mathrm{m}d\mathrm{R}}$ and $P_{\mathrm{m}q\mathrm{R}}$ for the rectifying converter.

Fig. 5 shows the control scheme for the grid-side inverting converter. The inverting converter is used to control the reactive power Q_{out} (measured at the 30 kV level) and the DC link voltage V_{DC}. The controlled reactive power is measured at the high voltage side of the individual FCWTG transformer (at the connection point to the 30 kV wind farm cable network shown in Fig. 2). The PI controllers for Q_{out} and V_{DC} define reference values for the dq-axis components $i_{d\mathrm{I}}$ and $i_{q\mathrm{I}}$ of the inverter AC current. The dq-axis components are in a reference frame oriented with the voltage at the high voltage side of the FCWTG transformer. Again the inner PI controllers define the dq-axis modulation indices $P_{\mathrm{m}d\mathrm{I}}$ and $P_{\mathrm{m}q\mathrm{I}}$ for the inverter.

It is worth noting that there are other options when choosing the control configuration for the converter system in an FCWTG [17]. The configuration chosen herein is what leads to the excess active power during a voltage dip being sent to the DC circuit. This power is dissipated by the braking resistor. In other configurations, the active power excess may cause large torque imbalances in the drive train, leading to unwanted mechanical system behaviour. The control system chosen herein does not cause these large torque imbalances, so a more detailed

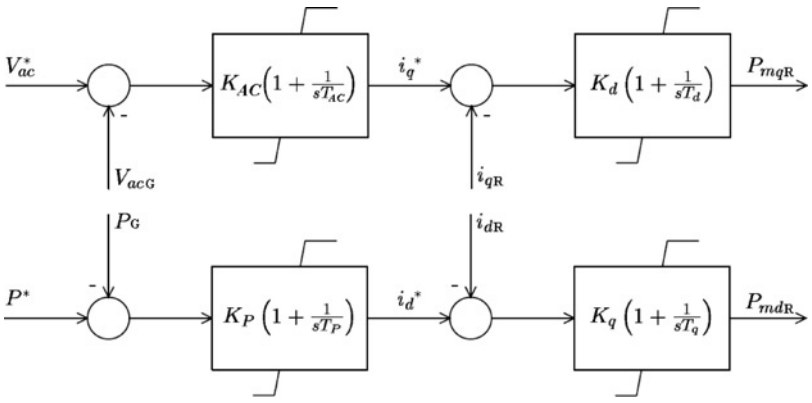

Figure 4 *Control of the machine-side rectifier*

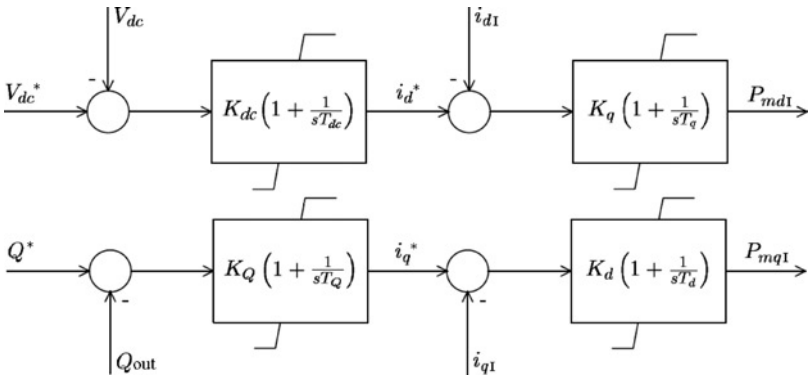

Figure 5 *Control of the grid-side inverter*

IET Renew. Power Gener., 2009, Vol. 3, No. 1, pp. 39–52
doi: 10.1049/iet-rpg:20070091

drive train model (as implemented in [18] or [19]) is not required.

3.1.1 Cross-coupling terms: According to [20], cross-coupling terms in the current control loops may or may not be implemented in commercial WTGs. In the literature, there are several examples of WTG control systems with cross-coupling terms [21–23] and also without cross-coupling terms [17, 24, 25]. The converter controllers used in this work do not have cross-coupling terms. Without the cross-coupling terms, it is easier to interpret the controller behaviour, and the results will show that the performance during transients is satisfactory.

3.1.2 Phase-locked loop: The *dq*-axis control system for converter currents requires that the phase angle of the AC voltage must be measured. This can be done using reference frame transformations [22, 23] or with a phase-locked loop (PLL) [17, 24]. In this work, the PLL method is chosen, since a PLL element is available in the library of PowerFactory.

3.2 Braking resistor control

Fig. 6 is a symbolic diagram of the control system used for the braking resistor. It is implemented as a user-defined component in PowerFactory using the simulation language DSL.

When the DC link voltage V_{DC} exceeds the maximum permitted value V_{max} (1.2 pu herein), the signal F_{BR} changes from 0 to 1. This causes the switch S_{BR} in Fig. 3 to close, inserting the braking resistor. With the braking resistor inserted, the sum of the exported active power and the braking resistor power is greater than the power supplied to the DC link circuit by the rectifying converter. This means that V_{DC} now begins to fall. When it falls below the minimum threshold V_{min} (1.15 pu herein), the signal F_{BR} returns to zero and the switch S_{BR} is opened again, removing the braking resistor. The voltage V_{DC} will now begin to rise again: leading to another switching action. This cycle of switching in and out the braking resistor continues until the disturbance ends; whereupon the braking resistor will no longer be required.

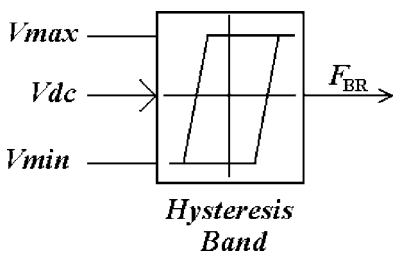

Figure 6 *Braking resistor control system*

3.3 Control system performance

Now that the control system has been explained, it is worth presenting an example of its performance before considering the aggregate modelling options. For this purpose, only one 5 MW FCWTG is modelled, with the high voltage of its transformer connected to the 30 kV bus in Fig. 2. A voltage dip is simulated that brings the voltage at the PCC (point of connection - see Fig. 2) down to 0.1 pu for 0.2 s. Fig. 7 is a graph of the PCC results. These results are the active and reactive power at the PCC, the PCC voltage and the current in per-unit measured at the PCC side of the wind farm transformer.

Fig. 7 shows that the performance of the FCWTG satisfies the requirements of the Irish grid code for this voltage dip. During the dip, the FCWTG continues to deliver active power to the grid and also supplies reactive power and the current is maximised at 1 pu. When the dip has ended, the active power quickly returns to its initial value. It is worth noting that the results shown in Fig. 7 agree favourably with those presented by the Enercon GmbH engineers for their FCWTG technologies in [6, 26]. To understand the influence of the braking resistor, Fig. 8 shows the results for the PMSM speed and the DC link voltage.

In continuous operation, the PLL will record a voltage phase angle that changes very little. This means that there is little disruption to the orientation of the *dq*-axis current controllers. During voltage dips, the measured voltage phase angle can change significantly, causing transients in the PLL. This is an unwanted disruption to the *dq*-axis current controllers, and it can compromise the FCWTG transient performance. To prevent this disruption, when a voltage dip is detected, the PLL is disabled, and the phase angle supplied to the *dq*-axis current controllers is equal to the measured phase angle before the voltage dip started. This means that the PLL dynamics are not influencing the FCWTG during the voltage dip.

When the voltage dip initially occurs, the active power that can be exported by the grid-side inverter is limited by the reduced AC voltage. The excess power that is produced by the PMSM flows into the DC link capacitor, causing the DC link voltage V_{DC} to rise. Recall from Section 3.1 that this is due to the choice of converter control configuration. When V_{DC} reaches V_{max}, the braking resistor is inserted. Then V_{DC} begins to fall and the braking resistor is disconnected when V_{DC} reaches V_{min}. This switching cycle continues as long as the voltage dip is present, as shown in Fig. 8. The application of braking resistors is this way has already been presented in [14, 27].

Another method of allowing FCWTGs to ride through grid faults involves the blocking of the converters [21]. Blocking means that the converters stop switching, so the active and reactive power can no longer be controlled. This is in violation of the Irish grid code requirements. By using

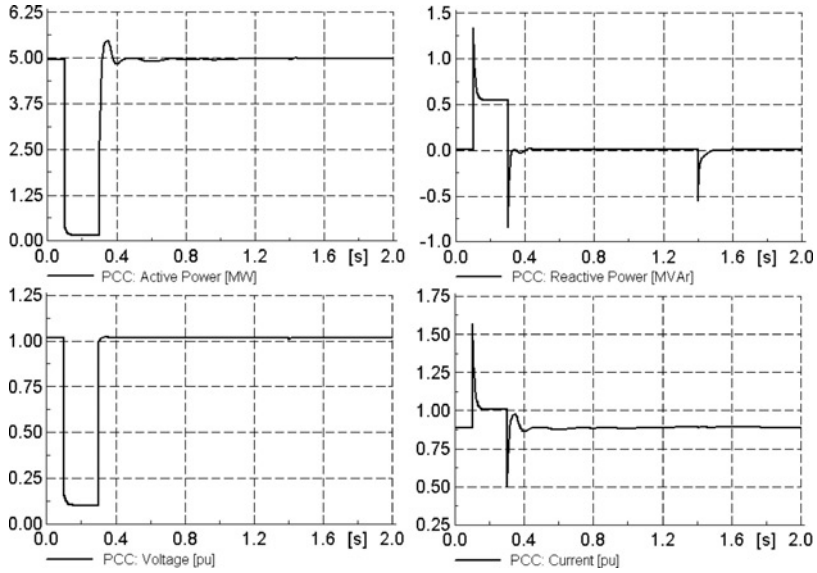

Figure 7 *PCC results for a single FCWTG*

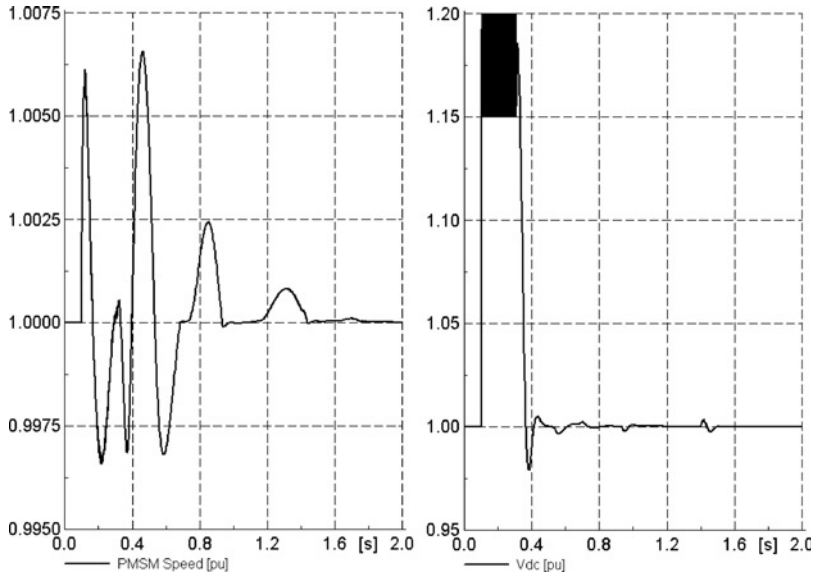

Figure 8 *PMSM speed and DC link voltage results for a single FCWTG*

the braking resistor, converter blocking is not required and the active and reactive power can be controlled during the voltage dip.

Some time after the voltage dip has ended (at $t = 1.4$ s in Fig. 7) the PLL is restored to active service, causing a minor blip which is only immediately evident in the reactive power output graph. Since this is quite a minor event, it will not be shown in the subsequent simulations.

The power dissipation by the braking resistor ensures that the PMSM can continue to produce rated power, meaning that the PMSM does not accelerate. This is evident in Fig. 8 where the PMSM speed changes by less than 1% during the voltage dip. This confirms that there is a negligible drive train stress due to the voltage dip, as predicted in Section 3.1. The insignificance of the speed deviations will be exploited in the development of aggregate models for this WTG concept.

4 Aggregate modelling options

Before discussing the various aggregate modelling options for the FCWTG employing braking resistor, it is useful to briefly discuss the aggregation options for fixed-speed WTGs. The final decision on the level of simplification for FCWTGs has very similar factors to the decision for fixed-speed WTGs. It will ultimately depend on whether or not the user wishes to represent the internal dynamics of the

IET Renew. Power Gener., 2009, Vol. 3, No. 1, pp. 39–52
doi: 10.1049/iet-rpg:20070091

wind farm, or just the active and reactive power results at the PCC.

4.1 Fixed-speed WTG aggregation

Fixed-speed WTGs are characterised by very small speed ranges from cut-in to rated power. This means that a reasonable assumption is that all WTGs in a fixed-speed wind farm are at the same speed, so the induction machines can be aggregated into one induction machine with rated power multiplied by the number of WTGs.

If the wind speed differences at the WTG locations in the wind farm are small, then the drive train models of the individual WTGs can also be aggregated. Hence, the wind farm is represented by one equivalent induction machine and one drive train which requires no parameter changes. This is the ultimate simplification level, and it is used in [28] for transient simulations.

If the wind speed differences cannot be neglected (as in a large wind farm with 80 WTGs [29]), there are two options to increase the modelling detail. In [28], the machine model remained aggregated but each drive train model was represented separately. This means that the active and reactive power output of the aggregate machine is adjusted to the wind speed differences but the speed deviations of the individual WTGs are not represented. In [29], the aggregate machine model was separated into several smaller aggregate machine models according to the profile of the wind speed deficit in the wind farm and several aggregate drive train models were used instead of individual ones. This method has the advantage of simulating WTG speed fluctuations more accurately, which may be important if overspeeding due to faults leads to individual disconnections.

In both models, the total active and reactive power output is accurately modelled. The choice of appropriate model depends on the accuracy with which one wishes to represent individual WTG speed fluctuations. This will also be the decisive factor for the FCWTG with braking resistor.

4.2 Variable-speed WTG aggregation

The simplest variable-speed aggregate model to construct is the one that represents the wind farm as a single WTG. This means that the electrical machine and the converters are scaled to the size of the wind farm. This is done by multiplying their rated powers by the number of WTGs in the wind farm. A single drive train model with no parameter changes is also used. This approach is used for variable-speed WTGs in [30] and is also used in [31] in combination with the aggregation technique for a fixed-speed wind farm presented in [29]. Another method of deriving an aggregate model for a variable-speed wind farm involves representing each WTG using a very simplified model [32, 33]. This approach does not allow for a reasonable comparison with a detailed model, so it is not considered herein.

In comparison to fixed-speed WTGs, the speed range of FCWTGs is large, owing to the maximum power-tracking strategy. This means that assuming that all FCWTGs in a wind farm are operating at the same speed is not so accurate. Since the output power of an FCWTG is a function of the generator speed fluctuations (maximum power tracking) as well as the wind speed, it is not appropriate to aggregate the PMSM models (assume equal speed) in a simulation investigating power fluctuations from the wind farm during continuous operation [28].

In a transient stability investigation, the simulation time is short, and the wind speed at each WTG is assumed to be constant. This suggests that a less complex model will suffice in this type of investigation. A number of aggregate modelling approaches are considered in this work, and the final choice will depend on whether the user wishes to represent internal wind farm dynamics during the simulation or whether the electrical behaviour at the point of connection is the only interest.

A further consideration in aggregate modelling is how to represent the impedance of the wind farm cable network. In [17], an approximate method is presented using short-circuit calculations for deriving the values of a series reactance that emulates the cable network. This reactance is placed in series with the wind farm transformer. However, the size of this reactance is much smaller than that of the leakage reactance of the wind farm transformer, so it may be neglected without significant loss in accuracy. This decision is also taken in [30, 32, 33].

4.3 Wind farm layout geometry

Fig. 2 is a PowerFactory diagram of the layout of the wind farm studied in this work. The wind speed vector $\vec{\mathbf{V}}_{\mathrm{W}}$, its angle θ_{V} and the numbering of the FCWTG locations are also shown. The wind farm contains 12 FCWTGs with 5 MW capacity each, totalling 60 MW. The FCWTG rotor diameter is 100 m, so a lattice spacing of 500 m is used between neighbouring FCWTG locations.

The instantaneous wind speed at each FCWTG location is constantly changing. However, in a transient stability simulation, the wind speed at each FCWTG is assumed to be equal to the mean wind speed. If there are significant differences in mean wind speed at the individual FCWTG locations, it can be attributed to the wake effect. Considering the wake effect means that different initial operating points for the individual FCWTGs can be established.

The wake effect also means that the output power from the wind farm is usually less than what one might expect by only

considering the incoming wind speed to the wind farm. In this aggregate modelling study, the wake effect calculations are used to initialise the wind farm at a reduced (less than expected) active power output and also to establish different initial operating points for the individual FCWTGs in the wind farm.

In [29], the author takes a simplified heuristic approach to the wake effect by changing the mean wind speed in each row of the studied wind farm and then representing the wind farm as rows of aggregate models. This approach only works when the wind speed angle θ_V is perpendicular to the rows (or columns) of the wind farm. In the more general case where the angle θ_V is arbitrary, the mean wind speed at each FCWTG location must be determined analytically and the results will not be so symmetric. In this work, the wake effect model presented in [34] is used to calculate the mean wind speed at each FCWTG location. The analytical method in [34] is comparable to the methodology employed in the industry standard tool WASP [35] that is used to estimate a wind farm's productivity. In [34], it has been shown that the wake effect is strongly dependent on the angle θ_V.

In this work, two wind conditions are considered. In the first case, the incoming wind speed $\overrightarrow{\mathbf{V}_W}$ has magnitude equal to the rated value (13.25 m/s, giving rated power output from the FCWTG) and an angle θ_V of 45°. In the second case, the incoming wind speed $\overrightarrow{\mathbf{V}_W}$ (magnitude 8.1 m/s) develops 50% rated power and has an angle θ_V of 75°. The resulting wake effects are shown in Table 1. The 'shadowed by' columns indicate which FCWTGs are being shadowed by the others in both cases. The wind speed columns indicate the wind speed V_{Wi} (in m/s) at each FCWTG location in both cases.

The wind farm wake factor c_{wake} is a measure of the reduction in wind farm power output due to the wake effect. This parameter is defined in (3)

$$c_{wake} = \frac{\text{Wind power including wake effect}}{\text{Wind power neglecting wake effect}} \quad (3)$$

When θ_V is 45°, only FCWTGs 7–8 and 11 and 12 are shadowed, and c_{wake} is ~94%. Table 1 shows that there are three unique wind speeds in the wind farm in this case, meaning that three aggregate models may be sufficient for the aggregation method of [29]. When θ_V is 75°, the amount of shadowing increases: now FCWTGs 2–4, 6–8 and 10–12 are shadowed. The result is that c_{wake} is now ~76%. The relationship between c_{wake} and θ_V is highly nonlinear [34]. The identical reduction in wind speeds at some FCWTG locations seen in Table 1 is a result of the uniform lattice spacing of the wind farm layout. If the spacing was more irregular, the number of unique wind speeds would increase. This suggests that the aggregation approach of [29] may not be so useful then. For visualisation purposes, Fig. 9 is a diagram of the shadowing arrangement in the first case.

5 Simulation results

The first wind farm model to consider is the one that represents each of the FCWTGs individually, henceforth referred to as the detailed model. The first case with a wind vector angle of 45° is chosen. Since the number of unique operating points is much less than the total number of FCWTGs, an aggregate model for the wind farm containing three aggregate FCWTGs (A, B and C) is studied, similar to the study of a fixed-speed wind farm in

Table 1 Wake calculation results

FCWTG	Shadowed by ($\theta_V = 45°$)	V_{Wi} ($\theta_V = 45^{\diamond}$)	Shadowed by ($\theta_V = 75°$)	V_{Wi} ($\theta_V = 75^{\diamond}$)
1	–	13.25	–	8.1
2	–	13.25	1	7.54
3	–	13.25	2	7.10
4	–	13.25	3	6.72
5	–	13.25	–	8.1
6	–	13.25	5	7.54
7	1	12.46	6	7.10
8	2	12.46	7	6.72
9	–	13.25	–	8.1
10	–	13.25	9	7.54
11	5	12.46	10	7.10
12	1,6,7	12.22	11	6.72

IET Renew. Power Gener., 2009, Vol. 3, No. 1, pp. 39–52
doi: 10.1049/iet-rpg:20070091

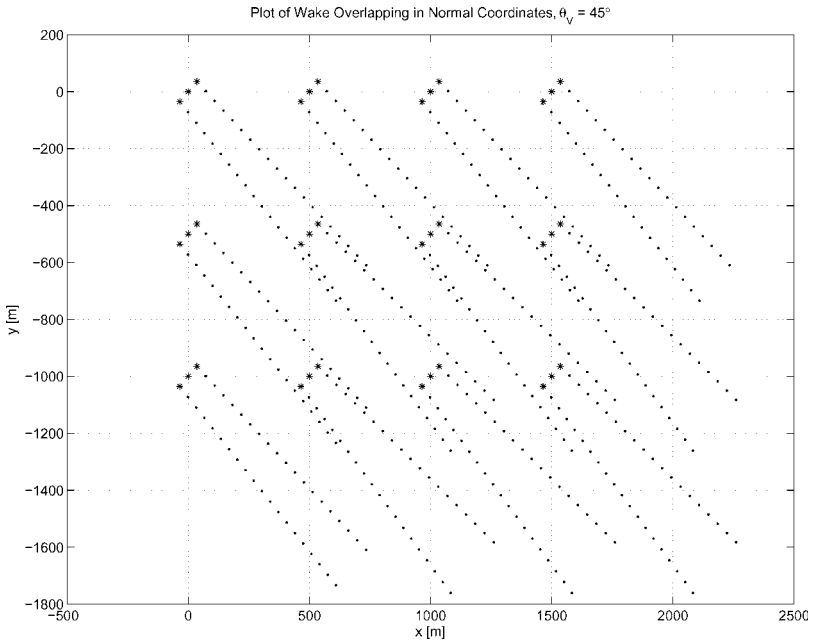

Figure 9 *Shadowing pattern in the first wind conditions case*

[29]. In the aggregate model, FCWTGs 1–6, 9 and 10 are represented as A; 7, 8 and 11 are represented as B and 12 is represented as C.

A voltage dip to 0.1 pu for 0.2 s was executed at the PCC busbar in Fig. 2. Fig. 10 shows a comparison of the simulations results at the PCC obtained using the detailed model and the three aggregate FCWTGs model. Fig. 11 shows a comparison of the PMSM speed and the DC link voltage results from both models.

Fig. 10 shows that the PCC results in both cases match very well. It also shows how the active power output is less than 60 MW due to the wake effect. In many cases, the PCC behaviour is as much information as is required: in a large-scale power system model the speed dynamics of the individual FCWTGs may not be of interest. Fig. 11 shows that the PMSM speed changes and DC link voltage results for FCWTG 7 (detailed model) and FCWTG B (aggregate model) agree very well, with the PMSM speed deviations being negligible (as in Section 3.3). Fig. 11 shows that there is a small difference in the initial PMSM speed of the detailed and aggregate models caused by the PowerFactory initialisation algorithm; but this is of little significance. It will now be shown that omitting the mechanical system from the FCWTG model will reduce the complexity without significantly compromising the accuracy of the PCC results.

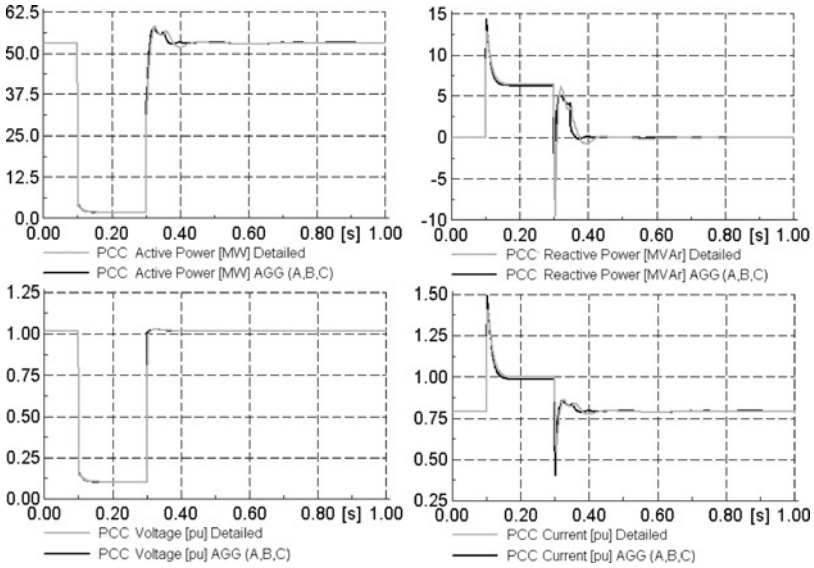

Figure 10 *Comparison of PCC results with detailed and aggregate models*

doi: 10.1049/iet-rpg:20070091

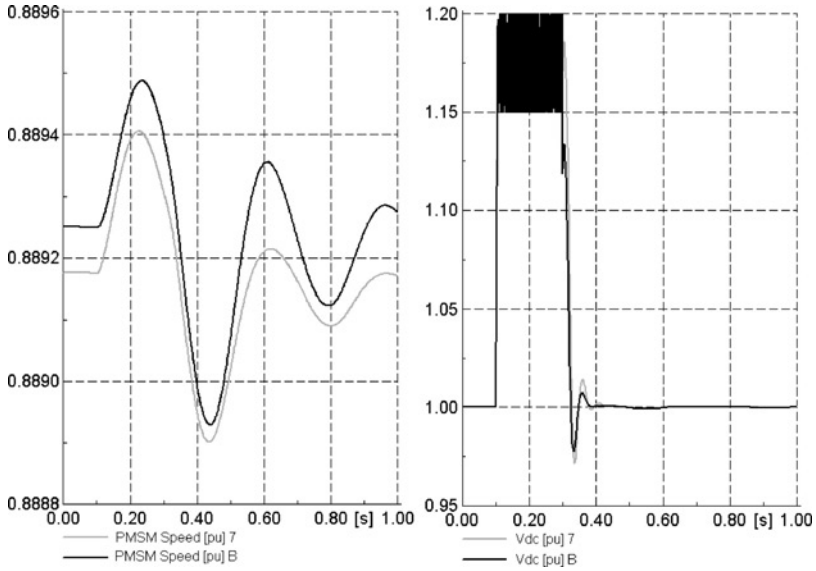

Figure 11 *Comparison of generator speed and DC link voltage*

5.1 Simplified aggregate model A

It has previously been demonstrated that the braking resistor ensures that FCWTG speed changes during voltage dips are negligible. This is because the supply of power to the DC circuit from the machine-side converter is approximately constant. So in terms of the PCC results, the FCWTG mechanical behaviour is not particularly relevant. So the model of the drive train, the PMSM and the machine-side converter, can be omitted. A constant power DC current source can be used to represent these instead (thus neglecting the machine side power fluctuations), and the simulation results at the PCC will not be greatly compromised. Fig. 12 shows the structure of this simplified model. The DC link voltage V_{DC} is fed back to calculate the current I_{DC} that keeps the active power supply constant.

A voltage dip to 0.1 pu for 0.2 s is again used to compare the results with those of the detailed model. Both wind conditions outlined in Table 1 will be investigated. When the mean wind speeds are calculated, the initial power of the individual generators can be deduced assuming maximum aerodynamic efficiency initially. These powers are then added together to get the initial power P_0 for the current source in the simplified model.

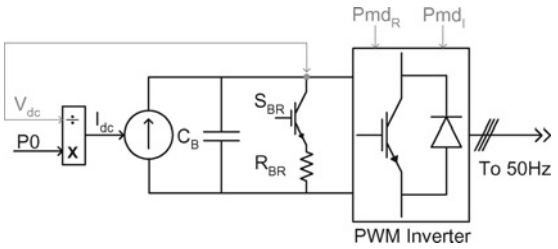

Figure 12 *Structure of the simplified aggregate model A*

Fig. 13 presents the simulation results using the first set of mean wind speed data. This shows that the PCC behaviour of the wind farm is still quite accurately represented by the simplified model with no machine side representation. However, the surge in active power output after the voltage dip has ended is over-estimated by this simplified aggregate model.

Fig. 14 presents the simulation results with the second set of mean wind speed data. In this case, the initial active power output of the wind farm is significantly below rated. Fig. 14 shows that the PCC behaviour of the wind farm in this case is also quite accurately represented by this simplified aggregate model. In this case, there is as even larger surge in active power after the voltage dip has ended. This is in fact due to the maximisation of the *d*-axis current of the grid-side inverter during the voltage dip, which does not diminish immediately after the voltage dip ends. This surge in active power output after the voltage dip has ended is now represented quite accurately by this simplified aggregate model.

5.2 Simplified aggregate model B

The simplified model presented in Section 5.1 still has a braking resistor in the DC circuit. The switching actions of the braking resistor are not reflected in the PCC result parameters. Therefore it seems logical to seek a model of the wind farm that does not include the braking resistor. This will provide further savings on computational complexity, and it will represent the ultimate level of modelling simplification when only the results at the PCC are required.

The model introduced in this section is a further simplification of the model used in the previous section. In this model, the DC link voltage is held constant by an

doi: 10.1049/iet-rpg:20070091

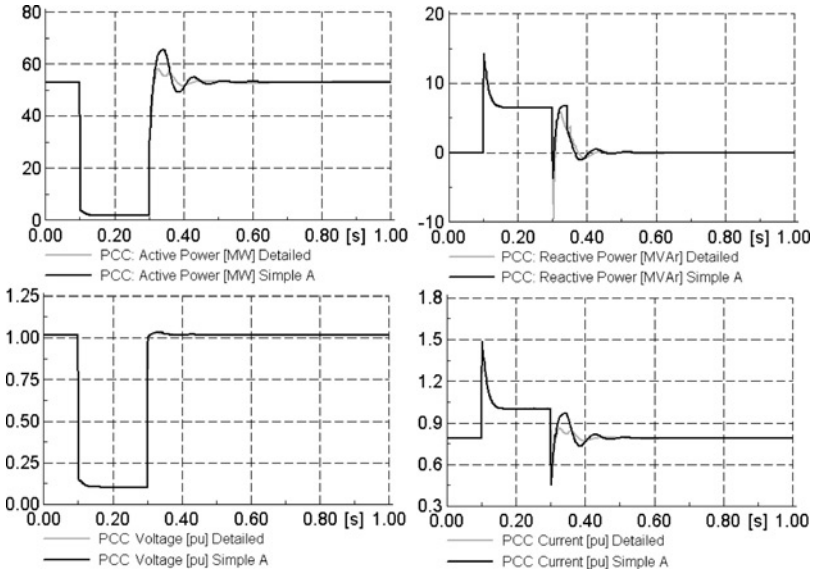

Figure 13 *PCC results for the detailed and simplified model A with rated incoming wind*

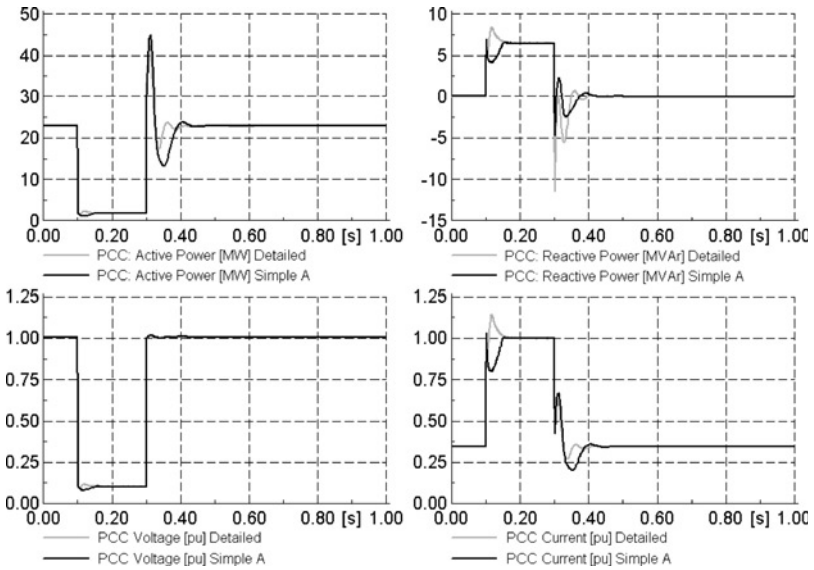

Figure 14 *PCC results for the detailed and simplified model A with 50% incoming wind*

infinite voltage source, with no capacitor or braking resistor present. The grid-side inverter is controlling the reactive power as usual, but now there is no control loop for the DC link voltage (as there is in Fig. 5).

Recall that when a voltage dip occurs, the grid-side converter increases its *d*-axis current to 1 pu, exporting as much active power as the dip voltage allows it to. This behaviour must be represented in this simplified model. Fig. 15 shows the modified grid-side inverter controller that emulates this behaviour.

In this figure, P_0 represents the initial active power at the beginning of the simulation, based on the assumption of constant wind speed (wind power) in the wind farm during the short simulation time frame. A filter is applied to the inverter AC voltage V_{AC}. The delay introduced by this filter is used to emulate the short delay in restoring the active power output of the FCWTG after the voltage dip has ended. The reference current i_d^* is calculated using these two parameters. When the AC input voltage drops, the reference current i_d^* increases, emulating the behaviour of the inverter and the DC link circuit in the detailed model. The filter is tuned so that the delayed response due to DC voltage dynamics in the detailed model is imitated.

Fig. 16 presents the PCC results from this model in comparison to the detailed model using the first set of mean wind speed data. These graphs show that this simplified model emulates the PCC behaviour of the wind farm quite accurately. It can very accurately model the initial overshoots of active and reactive power in this case,

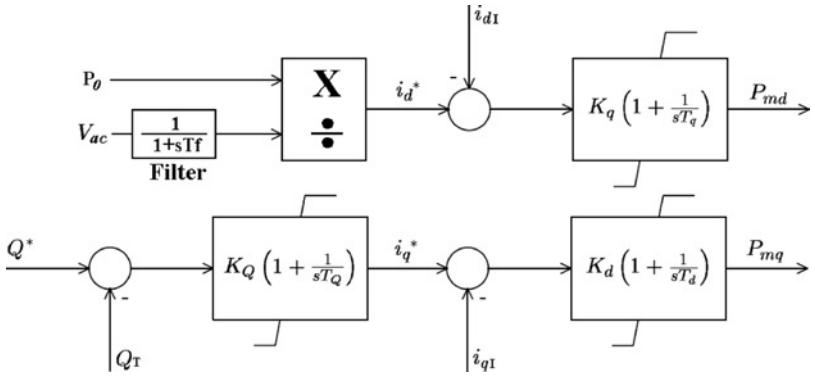

Figure 15 *Control of the grid-side inverter in the simplified aggregate model B*

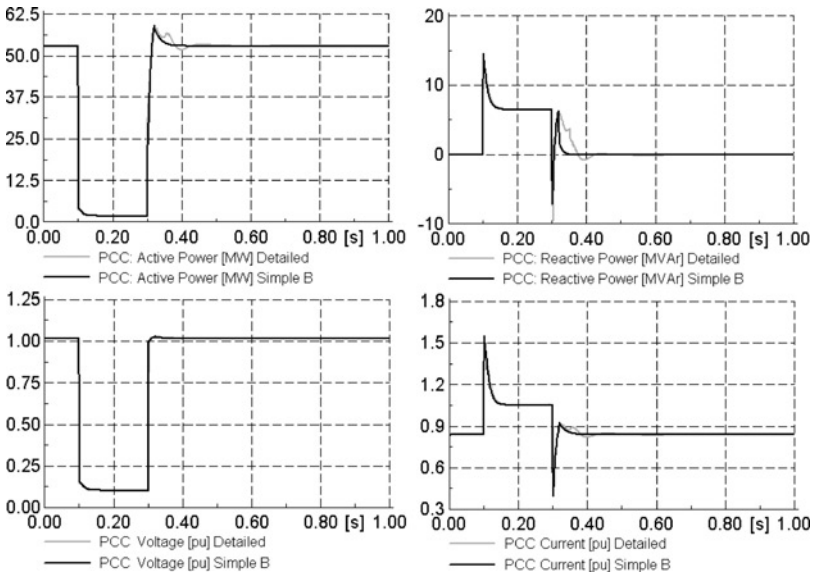

Figure 16 *PCC results for the detailed and simplified model B with rated incoming wind*

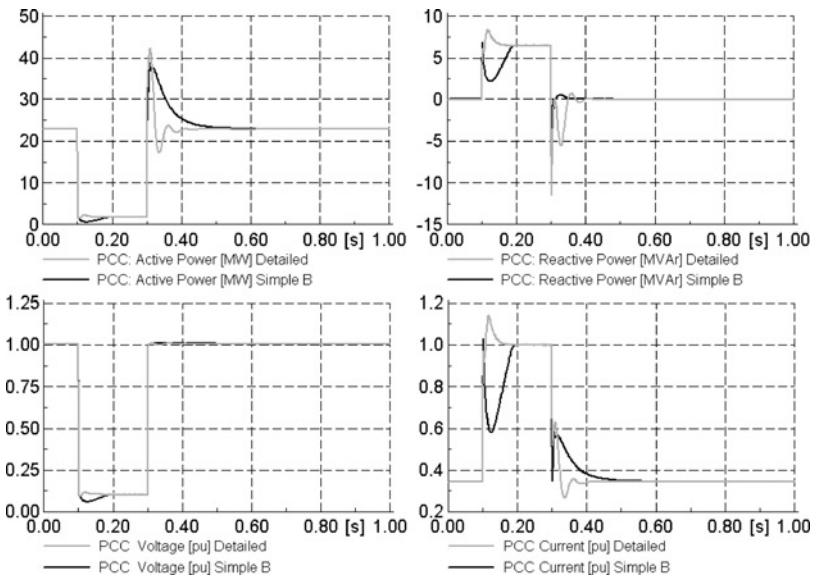

Figure 17 *PCC results for the detailed and simplified model B with 50% incoming wind*

IET Renew. Power Gener., 2009, Vol. 3, No. 1, pp. 39–52

doi: 10.1049/iet-rpg:20070091

which the previous simplified model did not do in its active power results. The small oscillations in powers after the dip are not so well represented, but this is a small compromise considering the increased saving on computation speed.

Fig. 17 presents the PCC results from this model in comparison to the detailed model using the second set of mean wind speed data. These graphs show that there are some inaccuracies in the PCC results in this case. This suggests that it might be better to use the model presented in Section 5.1 in this case.

6 Conclusions

In this paper, the transient behaviour of a wind farm containing FCWTGs subjected to a voltage dip has been investigated. A number of aggregate modelling options have been proposed and investigated. It has been shown that with a braking resistor included for ride-through purposes the speed deviations in the drive train are small. This leads to aggregate models that only represent the wind farm behaviour at the point of connection. Simplified aggregate models of the wind farm have been developed, which emulate the detailed model of the wind farm quite accurately, allowing a significant increase in simulation speed. This idea is crucially important in stability investigations of large power systems where a large number of wind farms may need to be modelled. Two simplified aggregate models have been presented, and it has been shown that in some cases one works better than the other, and vice-versa for other cases.

7 Future work

The power system model used herein contained one wind farm and a simple grid connection. It would be useful to test the accuracy of the aggregate models developed herein when they are applied to large-scale power system models containing several wind farms and possibly hundreds of WTGs.

Another application of aggregate modelling is wind farm representation during continuous operation. This topic has been investigated in [28]. It would be interesting to investigate the level of acceptable simplification of a wind farm model that can match the power fluctuation results of a detailed model. The averaging effect of individual WTG power fluctuations suggests that some simplifications are possible.

8 References

[1] HANSEN A., HANSEN L.: 'Wind turbine concept market penetration over 10 years (1995–2004)', *Wind Energy*, 2007, **10**, (1), pp. 81–97

[2] National Grid Electricity Transmission Std.: 'The grid code', http://www.nationalgrid.com/uk

[3] FERNANDEZ J.: 'Grid codes for wind energy in spain and developments in Europe'. Large Scale Integration of Wind Energy, Brussels, Belgium, November 2006

[4] ESB National Grid Std.: 'Wind farm power station grid code provisions', http://www.eirgrid.com

[5] E.On Netz GmbH Std.: 'Grid code: high and extra high voltage', September 2006

[6] HARTGE S., FISCHER F., WACHTEL S.: 'Experiences in dynamic behaviour of WEC and consequences for further developments'. Fifth Int. Workshop on Large-Scale Integration of Wind Power and Transmission Networks for Offshore Wind Farms, Glasgow, Scotland, April 2005, pp. 372–377

[7] DIgSILENT GmbH: http://www.digsilent.de/

[8] HEIER S.: 'Grid integration of wind energy conversion systems' (Wiley, 2006, 2nd edn.)

[9] PERDANA A., USKI-JOUTSENVUO S., CARLSON O., LEMSTRÖM B.: 'Comparison of an aggregated model of a wind farm consisting of fixed- speed wind turbines with field measurement', *Wind Energy*, 2008, **11**, (1), pp. 13–27

[10] AKHMATOV V.: 'Analysis of dynamic behaviour of electric power systems with large amounts of wind power'. PhD dissertation, Technical University of Denmark, Lyngby, Denmark, 2003, http://www.dtu.dk

[11] KRAUSE P., WASYNCZUK O., SUDHOFF S.: 'Analysis of electrical machinery and drive systems' (IEEE Press, 2002)

[12] JAUCH C.: 'Transient and dynamic control of a variable speed wind turbine with synchronous generator', *Wind Energy*, 2007, **10**, (3), pp. 247–269

[13] MICHALKE G., HANSEN A., HARTKOPF T.: 'Control strategy of a variable speed wind turbine with multipole permanent magnet synchronous generator'. European Wind Energy Conf., Milan, Italy, May 2007

[14] CONROY J., WATSON R.: 'Torsional damping control of gearless full-converter large wind turbine generators with permanent magnet synchronous machines', *Wind Eng.*, 2007, **31**, (5), pp. 325–340

[15] PIERIK J., MORREN J., WIGGELINKHUIZEN E., DE HAAN S., VAN ENGELEN T., BOZELIE J.: 'Electrical and control aspects of offshore wind farms II (Erao II) volume 1: dynamic models of wind farms'. ECN, Technical Report

[16] MOHAN N., UNDELAND T., ROBBINS W.: 'Power electronics: converters, drives and applications' (Wiley, 2002, 3rd edn.)

[17] PÖLLER M., ACHILLES S.: 'Direct drive synchronous machine models for stability assessment of wind farms'. 4th Int. Workshop on Large Scale Integration of Wind Power and Transmission Networks for OffShore Windfarms, Billund, Denmark, October 2003

[18] GH BLADED: 'Wind turbine design software', http://www.garradhassan.com

[19] LARSEN T., HANSEN A.: 'How to HAWC 2, the user's manual'. Risø National Laboratory, Roskilde, Denmark, Technical Report R-1597, December 2007

[20] AKHMATOV V.: 'Induction generators for wind power' (MultiScience, 2007)

[21] AKHMATOV V.: 'Modelling and ride-through capability of variable speed wind turbines with permanent magnet generators', *Wind Energy*, 2005, **9**, (4), pp. 312–326

[22] SUN T., CHEN Z., BLAABJERG F.: 'Transient stability of DFIG at an external short circuit fault', *Wind Energy*, 2005, **8**, (3), pp. 345–360

[23] PENA R., CLARE J., ASHER G.: 'DFIG using back-to-back PWM converters and its application to variable-speed wind-energy generation', *IET Electr. Power Appl.*, 1996, **143**, (3), pp. 231–241

[24] HANSEN A., JAUCH C., SØRENSEN P., IOV F., BLAABJERG F.: 'Dynamic wind turbine models in power system simulation tool DIgSILENT'. Risø National University, Roskilde, Denmark, Technical Report R-1400, December 2003

[25] HANSEN A., MICHALKE G.: 'Fault ride-through capability of DFIG wind turbines', *E. Renew. Energy*, **32**, (9), pp. 1594–1610

[26] HARTGE S., DIEDRICHS V.: 'Ride-through capability of Enercon wind turbines'. Fourth Int. Workshop on Large-Scale Integration of Wind Power and Transmission Networks for Offshore Wind Farms, Billund, Denmark, October 2003

[27] RAMTHARAN G., JENKINS N., ANAYA-LARA O.: 'Modelling and control of synchronous generators forwide-range variable-speed wind turbines', *Wind Energy*, 2007, **10**, (3), pp. 231–246

[28] PÖLLER M., ACHILLES S.: 'Aggregated wind park models for analysing power system dynamics'. 4th Int. Workshop on Large Scale Integration of Wind Power and Transmission Networks for OffShore Windfarms, Billund, Denmark, October 2003

[29] AKHMATOV V., KNUDSEN H.: 'An aggregate model of a grid-connected, large-scale, offshore wind farm for power stability investigations–importance of windmill mechanical system', *Electr. Power Energy Syst.*, 2002, **24**, (9), pp. 709–717

[30] SHAFIU A., ANAYA-LARA O., BATHURST G., JENKINS N.: 'Aggregated wind turbine models for power system dynamic studies', *Wind Eng.*, 2006, **30**, (3), pp. 171–186

[31] AKHMATOV V.: 'An aggregated model of a large wind farm with variable-speed wind turbines equipped with doubly-fed induction generators', *Wind Eng.*, 2004, **28**, (4), pp. 479–488

[32] SLOOTWEG J., DE HAAN S., POLINDER H., KLING W.: 'Aggregated modelling of wind parks with variable speed wind turbines in power system dynamic simulations'. 14 PSSC Conf., Seville, Spain, June 2002

[33] SLOOTWEG J., KLING W.: 'Aggregated modelling of wind parks in power system dynamic simulations'. IEEE PowerTech Conf., Bologna, Italy, June 2003

[34] KOCH F., GRESCH M., SHEWAREGA F., ERLICH I., BACHMANN U.: 'Consideration of wind farm wake effect in power system dynamic simulation'. IEEE PowerTech Conf., St Petersburg, Russia, June 2005

[35] WASP: 'Wind Atlas Analysis and Application Program', http://www.wasp.dk

doi: 10.1049/iet-rpg:20070091